

Two types of magnetism in the magnetic superconductor $\text{TmNi}_2\text{B}_2\text{C}$ U. Gasser^{a,*}, P. Allenspach^a, A. Furrer^b, A.M. Mulders^b^aLaboratory for Neutron Scattering, ETH Zürich and PSI, 5232 Villigen PSI, Switzerland^bInterfacultair Reactor Instituut, Delft University of Technology, Mekelweg 15, 2629 JB Delft, The Netherlands

Abstract

Crystal electric field (CEF) excitations of the R^{3+} -ions in $R\text{Ni}_2\text{B}_2\text{C}$ ($R=\text{Dy, Er, Ho, Tm}$) have been measured by inelastic neutron scattering (INS). From the data we have derived a consistent set of CEF-parameters. The parameters are in excellent agreement with measurements of the specific heat and the magnetic susceptibility. Our mean-field calculations of the size and the orientation of the magnetic moments are also in good agreement with measurements. From Mössbauer- and $\mu^+\text{SR}$ measurements it has been found that in the case of $\text{TmNi}_2\text{B}_2\text{C}$ there are two kinds of magnetic Tm-moments ($4.3 \mu_B$ and $0.1 \mu_B$). In this work we discuss a plausible explanation for the occurrence of small magnetic moments in $\text{TmNi}_2\text{B}_2\text{C}$ from the neutron scattering point of view. © 1998 Elsevier Science S.A.

Keywords: Quaternary borocarbides; Crystal field; Neutron scattering; Superconductor

1. Introduction

The ternary borocarbides with the composition $R\text{Ni}_2\text{B}_2\text{C}$ ($R=\text{rare earth}$) have some very interesting properties. They not only show various commensurate and incommensurate magnetic structures [1] of the R^{3+} -magnetic moments ($R=\text{Pr, Nd, Sm, Tb, Dy, Ho, Er, and Tm}$) but also coexistence of magnetism with superconductivity ($R=\text{Dy, Ho, Er, and Tm}$) and heavy fermion behaviour ($R=\text{Yb}$). In order to understand the magnetic properties of the borocarbides, information about the low temperature properties of the unfilled R^{3+} 4f-shell is needed, since these carry the magnetic moments. (The Ni-ions have been found to be nonmagnetic in these materials [1,2].) These properties are determined by the crystal electric field which causes a splitting of the 4f-shell states of the free ion.

Among other experimental techniques the properties of the 4f-shell have been studied by INS, neutron diffraction, Mössbauer spectroscopy and $\mu^+\text{SR}$ in this family of compounds. In the case of $\text{HoNi}_2\text{B}_2\text{C}$ and $\text{ErNi}_2\text{B}_2\text{C}$ the $\mu^+\text{SR}$ - and the neutron-results are in good agreement [3]. The precession frequency of the μ^+ confirms both the magnetic ordering temperatures (Table 1) and the moduli of the R^{3+} -magnetic moments that have been determined by neutron diffraction [1]. But in the case of $\text{TmNi}_2\text{B}_2\text{C}$ the $\mu^+\text{SR}$ measurements reveal a spontaneous internal

field of $0.1 \mu_B$ which is present up to about 30 K [3–5]. This contradicts both the magnetic ordering temperature ($T_m=1.5$ K) and the Tm^{3+} magnetic moment ($3.8 \mu_B$) determined by neutron diffraction [1]. Furthermore Mössbauer spectroscopy measurements on a $\text{TmNi}_2\text{B}_2\text{C}$ -sample of Mulders [6] which was also used for $\mu^+\text{SR}$ experiments revealed a small magnetic moment of $\sim 0.1 \mu_B$ of the Tm^{3+} -ions too. The first progress in understanding this contradiction between neutron diffraction and $\mu^+\text{SR}$ or Mössbauer was made when in a second Mössbauer-spectroscopy experiment the $\text{TmNi}_2^{11}\text{B}_2\text{C}$ -sample of Gasser (originally used for neutron CEF spectroscopy [7]) was measured. In this experiment two subspectra were observed at 0.3 K (Fig. 1(b)) [6]. Since the contributions of both spectra are high (20–25% and 75–80%) and the secondary phases of this sample are less than 5 wt.%, we believe that both subspectra originate from $\text{TmNi}_2\text{B}_2\text{C}$.

Table 1

Critical temperatures for the $R\text{Ni}_2\text{B}_2\text{C}$ compounds which show coexistence of magnetism with superconductivity ($R=\text{Dy, Ho, Er, and Tm}$). A comparison of calculated and measured magnetic moments is shown

R	T_c (K)	T_m (K)	T_N (K)	μ_{obs} (μ_B)	μ_{calc} (μ_B)	Direction	
						Obs.	Calc.
Dy	6	–	10.6	8.47(9)	9.8	(1,1,0)	(1,1,0)
Ho	8	8.5	5	8.62(6) (AF)	6.8	(1,1,0)	(1,1,0)
Er	11	6.8	–	7.19(10)	7.8	(1,0,0)	(1,0,0)
Tm	11	1.5	–	3.78(14)	4.7	(0,0,1)	(0,0,1)

T_m , T_N , and μ_{obs} were taken from Ref. [1].

*Corresponding author. Tel.: +41 56 310 3179; fax: +41 56 310 2939; e-mail: urs.gasser@psi.ch

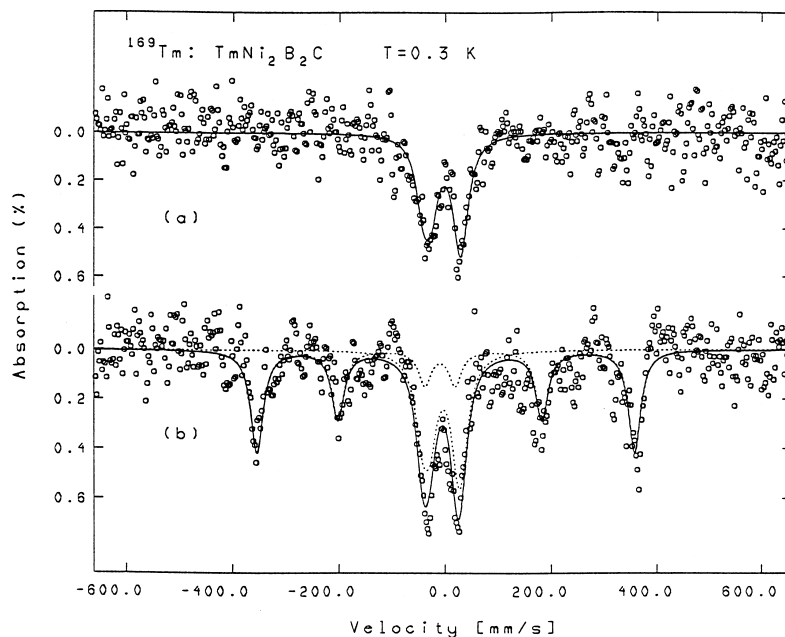


Fig. 1. ^{169}Tm Mössbauer spectra of the $\text{TmNi}_2\text{B}_2\text{C}$ sample of Mulders [6] (top) and of the $\text{TmNi}_{11}\text{B}_2\text{C}_{1.1}$ sample of Gasser (bottom) both measured at 0.3 K. (See text for details.)

The first subspectrum (20–25% of the total intensity) consists of a quadrupole doublet with a small broadening which corresponds to a magnetic moment of approximately $0.1 \mu_{\text{B}}$. This is the kind of spectrum that was already observed in the sample of Mulders (Fig. 1(a)). The second subspectrum (75–80% of the total intensity) contains a sextuplet which corresponds to an ordered magnetic Tm^{3+} moment of $4.3(1) \mu_{\text{B}}$. Therefore there are two kinds of magnetic Tm^{3+} moments coexisting in this sample of $\text{TmNi}_2\text{B}_2\text{C}$.

Different ratios of starting materials were used for the synthesis of the two samples. The ratios were $\text{Tm}:\text{Ni}:\text{B}:\text{C}=1.1:2:2:1$ for Mulders' sample and $\text{Tm}:\text{Ni}:\text{B}:\text{C}=1:2:2:1.1$ for the second sample. Therefore the difference in carbon content could possibly account for the different magnetic behaviour. In Ref. [6] Mulders et al. have argued that Tm ions near a carbon vacancy carry a small magnetic moment of about $0.1 \mu_{\text{B}}$ whereas the large magnetic moment ($4.3(1) \mu_{\text{B}}$) is present on Tm-ions with all four nearest neighbour carbon ions. The carbon vacancies modify the CEF at the Tm-site and therefore influence the Tm 4f magnetism. The inability of the μ^+ SR technique to detect the large Tm magnetic moment can be explained with this model. Apart from the unoccupied carbon sites CeRu_2Si_2 has the same chemical structure as $\text{TmNi}_2\text{B}_2\text{C}$, and from μ^+ SR experiments it is known that the μ^+ occupies the empty carbon site. Therefore it is most probable that the carbon site in $\text{TmNi}_2\text{B}_2\text{C}$ is preferred by the μ^+ if it is empty. This would mean that μ^+ SR experiments are much more sensitive for Tm-ions next to carbon vacancies which are present in most samples.

2. CEF of $\text{TmNi}_2\text{B}_2\text{C}$

In an earlier work [7] we have used INS in order to measure CEF transitions in the compounds with $R=\text{Ho}$, Er, and Tm. By fitting the neutron CEF cross-section to the measured data we were able to extract a consistent set of CEF parameters which determine the CEF hamiltonian $\mathbf{H}_{\text{CEF}}=\sum_{n,m} A_{nm} \mathbf{Y}_n^m$ (Table 2). The eigen-energies and eigen-states of the 4f-shell, the magnetic contribution to the specific heat and the magnetic susceptibility can be calculated when \mathbf{H}_{CEF} is known. Furthermore the CEF parameters found from the fits for $R=\text{Ho}$, Er, and Tm were extrapolated to the other rare earths ($R=\text{Pr}$, Nd, Sm, Tb, Dy, and Yb) [8]. For these compounds and for $R=\text{Ho}$, Er, and Tm we have estimated the direction and modulus of the magnetic moment in the ordered state with mean field calculations [7,8]. The good agreement of these calculations with the measurements throughout the rare earth series is strong evidence for the correctness of our CEF model. Furthermore our CEF parameters reproduce the ^{169}Tm quadrupole splitting of the $4.3 \mu_{\text{B}}$ -phase which is known from Mössbauer measurement. Therefore we

Table 2
CEF parameters (in meV) of $\text{RNi}_2\text{B}_2\text{C}$ ($R=\text{Ho}$, Er, Tm)

	ErNi_2B_2	$\text{HoNi}_2\text{B}_2\text{C}$	$\text{TmNi}_2\text{B}_2\text{C}$
A_{20}	-14.5 ± 6	-6.3 ± 1.3	-13.0 ± 0.3
A_{40}	2.3 ± 0.8	3.3 ± 0.3	2.16 ± 0.14
A_{44}	-71.4 ± 3.3	-73.9 ± 1.3	-63.1 ± 1.2
A_{60}	-0.42 ± 0.3	-0.61 ± 0.12	-1.32 ± 0.05
A_{64}	11.7 ± 1.4	10.1 ± 3.1	15.6 ± 1.1

believe that the CEF model presented in Refs. [7,8] correctly describes the single-ion magnetism of the Tm-ions with a magnetic moment of $\sim 4.3 \mu_B$.

3. Neutron scattering results on $\text{TmNi}_2^{11}\text{B}_2\text{C}_x$

In order to learn more about the coexistence of two different magnetic moments in $\text{TmNi}_2\text{B}_2\text{C}$ we have prepared $\text{TmNi}_2^{11}\text{B}_2\text{C}_x$ samples with different initial carbon contents ($x=0.75, 0.85, 1.00, 1.20$). The samples were prepared by standard arc melting technique [9]. The starting materials were mixed and pressed to pellets. These were melted several times for about 10 s. During the melting process a part of the more volatile elements (mainly carbon) is lost. In order to compensate for this effect some extra carbon can be added. (In the case of the sample with initial carbon content $x=1.20$ some of the extra carbon was expelled during melting and formed a black coating on the surface of the sample. This coating was removed by sandblasting.) After melting the samples were wrapped in Ta-foil and sealed in quartz ampoules under vacuum and were annealed for several days at $(1050 \pm 10)^\circ\text{C}$. After grinding the samples to fine powder their quality was checked by X-ray (all samples) and neutron diffraction ($x=0.85, 1.20$). The samples with $x < 1$ contain large amounts of additional phases, while the other two samples are essentially single phase (additional phases less than 5 wt.%). The characterization of the four new samples and the older $\text{TmNi}_2\text{B}_2\text{C}_{1.1}$ sample is summarized in Table 3. According to the simple carbon vacancy model all Tm-ions with less than four nearest neighbour C-ions contribute to the $0.1 \mu_B$ -phase. Therefore it is expected from the 99% occupation of the carbon sites in the $\text{TmNi}_2^{11}\text{B}_2\text{C}_{1.1}$ sample that only 4% of the Tm-ions contribute to the $0.1 \mu_B$ -phase in this sample. This is much less than the value of 20–25% observed by Mössbauer spectroscopy.

CEF spectroscopy measurements were performed for all samples on the triple-axis spectrometer IN3 at ILL (Grenoble, France). If the carbon vacancy model is correct, there should be CEF transitions in addition to the ones of the $4.3 \mu_B$ -phase when not all carbon sites are occupied. In the samples $\text{TmNi}_2^{11}\text{B}_2\text{C}_{0.85}$, $\text{TmNi}_2^{11}\text{B}_2\text{C}_{1.10}$, and

$\text{TmNi}_2^{11}\text{B}_2\text{C}_{1.20}$ it is expected that 84%, 96%, and 100%, respectively, of the Tm-ions contribute to the $4.3 \mu_B$ -phase. From Fig. 2 and from the CEF parameters listed in Table 4 it can be seen that the observed CEF spectra change only very little when x is changed from 0.75 to 1.20. As in our previous work [7,8] the CEF transitions of the $4.3 \mu_B$ -phase are observed. Only for $x=0.75$ and 0.85 there is a small additional peak at about 7.5 meV, which is

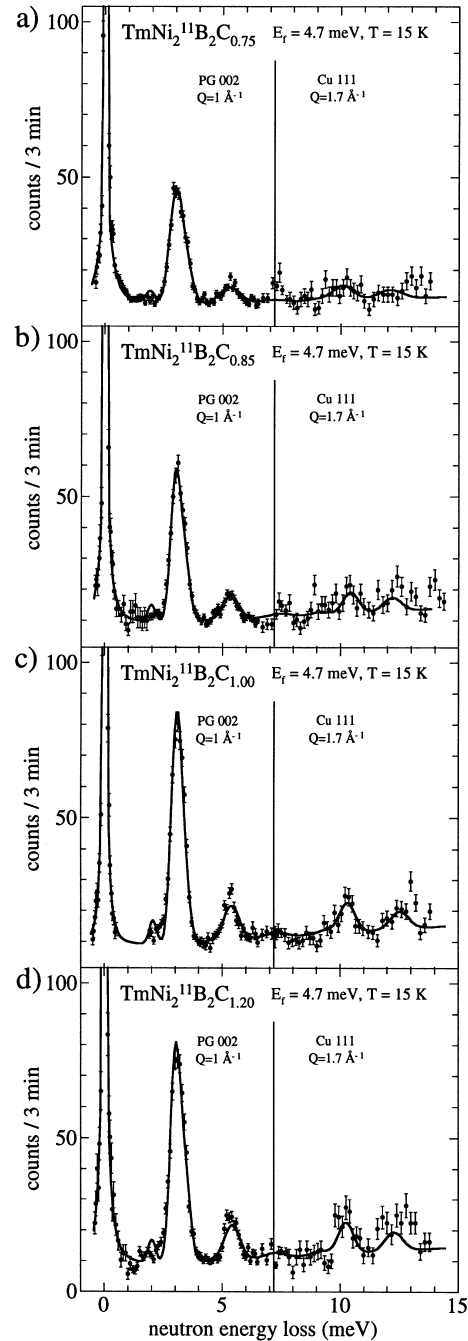


Fig. 2. Neutron CEF-spectra of $\text{TmNi}_2^{11}\text{B}_2\text{C}_x$ samples ($x=0.75, 0.85, 1.00, 1.20$) taken on the triple-axis instrument IN3 (ILL, Grenoble) in the paramagnetic state. The lines result from CEF profile fits of the $4.3 \mu_B$ -phase to the data.

Table 3
Characterization of $\text{TmNi}_2\text{B}_2\text{C}_x$ samples ($x=0.75, 0.85, 1.00, 1.10, 1.20$). The occupations of the Ni-, B-, and C-sites are given relative to the occupation of the Tm-site. In the last column the known secondary phases are listed together with their amount (in weight %).

Sample	$c_{\text{Ni}}/c_{\text{Tm}}$	$c_{\text{B}}/c_{\text{Tm}}$	$c_{\text{C}}/c_{\text{Tm}}$	Secondary phases
$\text{TmNi}_2^{11}\text{B}_2\text{C}_{0.75}$	—	—	—	$\text{TmNi}_4\text{B} \sim 20\%$
$\text{TmNi}_2^{11}\text{B}_2\text{C}_{0.85}$	1.94	1.93	0.96	$\text{TmNi}_4\text{B} \sim 10\%$
$\text{TmNi}_2^{11}\text{B}_2\text{C}_{1.00}$	—	—	—	Unknown $\sim 5\%$
$\text{TmNi}_2^{11}\text{B}_2\text{C}_{1.10}$	1.97	1.97	0.99	$\text{Ni}_2\text{B} 0.5\%$
$\text{TmNi}_2^{11}\text{B}_2\text{C}_{1.20}$	1.98	1.96	1.00	$\text{Ni}_2\text{B} 2\%$

Table 4

CEF parameters (in meV) for the $4.3 \mu_B$ -phase of $\text{TmNi}_2\text{B}_2\text{C}_x$ ($x=0.75, 0.85, 1.00, 1.20$)

	$\text{TmNi}_2^{11}\text{B}_2\text{C}_{0.75}$	$\text{TmNi}_2^{11}\text{B}_2\text{C}_{0.85}$	$\text{TmNi}_2^{11}\text{B}_2\text{C}_{1.00}$	$\text{TmNi}_2^{11}\text{B}_2\text{C}_{1.20}$
A_{20}	-14.8 ± 0.6	-13.7 ± 0.4	-12.4 ± 0.5	-12.3 ± 0.4
A_{40}	2.4 ± 0.3	2.0 ± 0.2	2.0 ± 0.2	1.9 ± 0.2
A_{44}	-65.4 ± 2.3	-63.8 ± 1.6	-60.3 ± 1.7	-59.8 ± 1.7
A_{60}	-1.33 ± 0.07	-1.45 ± 0.05	-1.39 ± 0.04	-1.43 ± 0.05
A_{64}	11.2 ± 2.5	12.2 ± 1.5	15.8 ± 1.6	14.6 ± 1.7

too small to account for a contribution of 16% of the Tm-ions. Next to this peak only a change of the intensity is observed. If it is assumed that only the $4.3 \mu_B$ -phase is present in $\text{TmNi}_2^{11}\text{B}_2\text{C}_{1.20}$ and the 3 meV peak is normalized for comparison one obtains for $x=0.75, 0.85, 1.00$, and 1.20 a $4.3 \mu_B$ -phase contribution of 79%, 80%, 97%, and 100%, respectively. These values are in rather good agreement with the above mentioned expectations from the simple carbon vacancy model. But the absence of a clear second set of CEF transitions which could belong to the $0.1 \mu_B$ -phase indicates that probably the situation is more complicated. It is possible that not one distinct but several CEF surroundings belong to the Tm-ions with the small magnetic moment. In this case these many additional CEF transitions are too weak to be distinguished from the background. Since carbon and the isotope ^{11}B have almost the same coherent neutron scattering length, carbon–boron disorder cannot be excluded with neutron diffraction and it might be related to the $0.1 \mu_B$ -phase.

For a more detailed analysis of the coexistence of the two kinds of magnetic moments in $\text{TmNi}_2\text{B}_2\text{C}$, Mössbauer spectroscopy data of the same samples will be very useful. These measurements will be published elsewhere.

References

- [1] J.W. Lynn, S. Skanthakumar, Q. Huang, S.K. Sinha, Z. Hossain, L.C. Gupta, R. Nagarajan, C. Godart, Phys. Rev. B 55 (1997) 6584.
- [2] B.J. Suh, F. Borsa, D.R. Torgeson, B.K. Cho, P.C. Canfield, D.C. Johnston, J.Y. Rhee, B.N. Harmon, Phys. Rev. B 53 (1996) 6022–6025.
- [3] L.P. Le, R.H. Heffner, G.J. Nieuwenhuys, P.C. Canfield, B.K. Cho, A. Amato, R. Feyerherm, F.N. Gygax, D.E. MacLaughlin, A. Schenck, Physica B 206–207 (1995) 552–554.
- [4] D.W. Cooke, J.L. Smith, S.J. Blundell, K.H. Chow, P.A. Pattenden, F.L. Pratt, S.F.J. Cox, S.R. Brown, A. Morobel-Sosa, R.L. Lichti, L.C. Gupta, R. Nagarajan, Z. Hossain, C. Mazumdar, C. Godart, Phys. Rev. B 52 (1995) R3864.
- [5] A. Amato, P.C. Canfield, B.K. Cho, R. Feyerherm, F.N. Gygax, R.H. Heffner, L.P. Le, D.E. MacLaughlin, G.J. Nieuwenhuys, A. Schenck, unpublished.
- [6] A.M. Mulders, P.C.M. Gubbens, U. Gasser, C. Baines, K.H.J. Buschow, subm. to Phys. Rev. B, May 1997.
- [7] U. Gasser, P. Allenspach, F. Fauth, W. Henggeler, J. Mesot, A. Furrer, S. Rosenkranz, P. Vorderwisch, M. Buchgeister, Z. Phys. B 101 (1996) 345–352.
- [8] U. Gasser, P. Allenspach, J. Mesot, A. Furrer, Physica C 282–287 (1997) 1327.
- [9] M. Buchgeister, A. Handstein, J. Klosowski, N. Mattern, P. Verges, U. Wiesner, Mater. Lett 22 (1995) 203.